RRR-robot design : basic outlines, servo sizing, and control

Proceedings of the 1997 IEEE International
Conference on Control Applications
Hartford, CT • October 5-7, 1997

RRR-robot design: basic outlines, servo sizing, and control

Bert van Beek* and Bram de Jager
Faculty of Mechanical Engineering, Eindhoven University of Technology
P.O. Box 513, 5600 MB Eindhoven, The Netherlands

Abstract

The RRR-robot project aims at a manipulator-like system (with three rotational degrees of freedom), to test a variety of advanced nonlinear control strategies. Since for high-speed tracking of complex trajectories, Coriolis and centrifugal torques form an essential part of the occurring nonlinear effects, the main requirement of this robot is to highlight these velocity dependent torques.

In this paper the outlines of the manipulator design are discussed. By exploring the main requirements two important features of the RRR-robot are introduced: unconstrained rotation in each link (e.g., by using sliprings) and the use of direct-drive servos. Several types of direct-drive servos are discussed and a choice is made to use brushless direct-current motors. The iterative dynamic optimization problem of choosing appropriate servos is solved by using a rigid-robot model implemented in a symbolic manipulation program. This program is also used for simulation and evaluation of both open and closed loop behavior.

Keywords: robot design, direct-drive motor, nonlinear system control.

1. Introduction

Industrial robots Robots are applied in a great variety of fields, of which industrial automated manufacturing is an important one. Objectives such as reducing the manufacturing costs, increasing the productivity, and improving the product quality standards, represent the main factors that have promoted an increasing use of robotics technology. Nowadays, typical robot applications include: materials handling (e.g., palletizing or packaging), manipulation (e.g., arc welding or spray painting), and measurement (e.g., object inspection).

Not surprisingly, there is an increasing demand from industry for systems which can achieve these tasks faster and/or more accurately. Increased accuracy may result in a reduction of post processing steps, and the increase of velocity obviously increases throughput. If this increase of performance can be achieved at the same price or lower, both improvements will result in lower price per product.

In order to achieve fast response times in combination with an acceptable effort (i.e., driving torque), industrial manipulators should be lightweight constructions. However, lightweight robot arms are also flexible. Especially at high velocities, deformations and vibrations can occur in both the joints and the links. These unwanted dynamics seriously reduce a robot's accuracy. In applications which require precise tracking of a moving position reference, such as arc welding, laser cutting or, gluing, this is a real problem.

One way to avoid such unwanted dynamics is realizing a stiff construction, i.e., stiff joints and stiff arms. Designing both stiff and lightweight manipulators, though, is a difficult engineering task.

Stiff behavior by control An alternate approach is letting the construction "behave stiffly" by using advanced control strategies to deal with the flexibilities in manipulator joints and/or links. Unlike conventional control designs, these strategies do not assume stiff and rigid behavior but are based on models describing the flexible components. For fast industrial robots, velocity dependent torques (like Coriolis and centrifugal torques) are expected to play a decisive role in these models.

Due to rapid developments in computing hardware, the application of more complex and nonlinear control algorithms has become much less a constraint. However, implementations of control strategies based on flexible models are still rare in industrial robots [4].

Objective RRR-robot The objective of the RRR-robot[1] project is to realize a manipulator-like system to test these advanced nonlinear control strategies. To achieve a resemblance with conventional industrial robots (e.g., Puma-type robots), the system should have a chain structure and at least three rotational degrees of freedom. As Coriolis and centrifugal torques play an important role in many of the proposed model-based control concepts, the main requirement of the robot is the ability to maintain these torques at a significant level.

Outline of this paper In Section 2 the problem which the RRR-robot aims to solve is analyzed, and some relevant design specifications are summarized. After choosing an appropriate servo motor type, the problem of servo sizing is discussed in Section 3. Section 4 provides a design evaluation with closed loop simulation, while section 5 concludes with some remarks.

2. Experimental validation problem

For high-speed tracking of complex trajectories, Coriolis and centrifugal torques form an essential part of the nonlinear terms. Therefore, these terms play an important role in many of the proposed control strategies (e.g., [1]) For testing and further development of these controllers, experiments are necessary. The main problem, however,

*contacting author: Telephone: +31 40 2472827, Fax: +31 40 2461418, Email: bert@wfw.wtb.tue.nl

[1] The triple R stands for three rotational degrees of freedom.

0-7803-3876-6/97 $10.00 © 1997 IEEE

is to highlight the Coriolis and centrifugal torques. For experimental validation, these velocity dependent torques should be kept significantly large during a considerable period. In most industrial manipulators, these demands encounter two fundamental problems:

- the rotation of each joint is constrained to a certain angle due to the cables used for energy and data transport throughout the manipulator;
- the presence of gears with high reduction ratios (e.g., harmonic drives) tends to linearize the system dynamics.

To illustrate these problems, consider a completely rigid manipulator model (rigid joints and links). Without flexibility, friction, or backlash, the equations of motion are given by

$$M(\underline{q})\,\ddot{\underline{q}} + C(\underline{q},\dot{\underline{q}})\,\dot{\underline{q}} + \underline{g}(\underline{q}) = \underline{\tau} \tag{1}$$

where $\underline{q}$ denotes the vector with rotation angles, $\dot{\underline{q}}$ the angular velocities, and $\ddot{\underline{q}}$ the angular accelerations. So the torques $\underline{\tau}$ acting on each link consist of inertia torques, $M(\underline{q})\,\ddot{\underline{q}}$, Coriolis and centrifugal torques, $C(\underline{q},\dot{\underline{q}})\,\dot{\underline{q}}$, and torques due to gravity $\underline{g}(\underline{q})$.

Constrained rotations In order to highlight the Coriolis and centrifugal torques for any link i, the contribution $\{C(\underline{q},\dot{\underline{q}})\,\dot{\underline{q}}\}_i$ to the total torque τ_i should be substantial during a sufficiently long period of time. To quantify this requirement, the following integral ratio is defined:

$$r_i = \frac{\int_0^\infty \mid \{C(\underline{q},\dot{\underline{q}})\dot{\underline{q}}\}_i \mid d\xi}{\int_0^\infty \mid \tau_i \mid d\xi}. \tag{2}$$

Highlighting the Coriolis and centrifugal torques now means achieving a large ratio. As can be seen in (1), this requires a combination of high velocities and low accelerations. If the joint rotation angles are limited, such a combination can be achieved only with considerable energy and only over a short period of time, since shortly after the acceleration to a certain velocity, the de-acceleration must begin in order to avoid breaking any cables.

Transmissions To understand the linearizing effect of transmissions, first, they must be included in the model. Assume the transmissions are rigid and without backlash. Let $\underline{q}_m$ and $\underline{\tau}_m$ denote the vectors of joint actuator displacements and actuator driving torques respectively; the transmissions then establish the following relationships:

$$\begin{cases} \underline{q}_m = K_r\,\underline{q} \\ \underline{\tau}_m = K_r^{-1}\underline{\tau} \end{cases} \tag{3}$$

where K_r is a diagonal matrix containing the gear reduction ratios k_{r_i}. The moments of inertia, I_{m_i}, of each motor with respect to its rotor axis are collected in the diagonal matrix I_m.

Now the *mass matrix* $M(\underline{q})$ can be split into a constant diagonal matrix, $K_r I_m K_r$, and a configuration-dependent (dependent on functions of $\underline{q}$) matrix $\Delta M(\underline{q})$, i.e.,

$$M(\underline{q}) = K_r I_m K_r + \Delta M(\underline{q}). \tag{4}$$

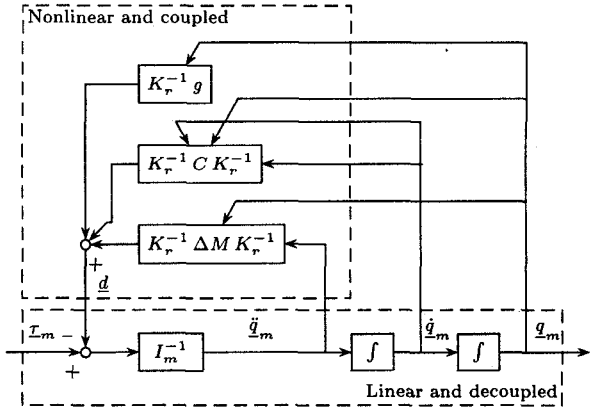

Figure 1: Block scheme of a rigid manipulator with transmissions.

Substituting (3) and (4) into (1) yields

$$\underline{\tau}_m = I_m\,\ddot{\underline{q}}_m + \underline{d} \tag{5}$$

where

$$\begin{aligned} \underline{d} =& K_r^{-1}\,\Delta M(\underline{q}) K_r^{-1}\,\ddot{\underline{q}}_m + K_r^{-1}\,C(\underline{q},\dot{\underline{q}})\,K_r^{-1}\,\dot{\underline{q}}_m \\ &+ K_r^{-1}\underline{g}(\underline{q}) \end{aligned} \tag{6}$$

represents the contribution depending on the configuration. As illustrated by the block scheme of Fig. 1, the system described by (1) actually consists of two subsystems:

1. a linear and decoupled subsystem in which each component of $\underline{\tau}_m$ influences only the corresponding component of $\underline{q}_m$,
2. a nonlinear and coupled subsystem.

In case of high reduction gears ($k_{r_i} \gg 1$), the contribution of the nonlinear interaction term $\underline{d}$ is small, and can be considered as a disturbance for each joint servo. As a result the integral ratio of Eq. (2) becomes small, since the torque τ_i is almost completely determined by the motor inertia.

The price to pay, however, for using transmissions is the occurrence of joint friction, elasticity, and backlash that may limit system performance more than the nonlinear terms. The use of drives without transmissions, *direct-drives* ($K_r = I$), could eliminate these drawbacks, but the influence of nonlinearities and coupling between the joints then becomes relevant. Aside from the cost and size of direct-drives, this is the main reason that these servos are not yet popular in industrial manipulators [5].

Summary Analyzing the experimental control system validation problem with conventional industrial robots, and thus exploring the main requirement (maintaining high Coriolis and centrifugal torques) two sub-problems were identified:

- the joint rotations are constrained, and

- the transmissions have high reduction rates.

In the RRR-robot, these problems should be solved, leading to:

- the removal of constraints on the rotation of each joint, and
- the use of transmissions with small, unity (direct-drive servos) or even inverse reduction rates ($k_{r_i} < 1$).

3. Joint actuation system

The RRR-robot can be divided into several subsystems, which are partly independent of each other. In its turn, each subsystem can be divided into several components. Here the focus is on choosing an appropriate joint actuation system consisting of transmissions and servo motors (with power supplies and power amplifiers). Other subsystems (see Fig. 2) are also needed:

- a measurement system for determining
  - the joint states (e.g., joint angles),
  - the link states (e.g., with strain gages for flexible links), and
  - the Cartesian position of the end-effector;
- a control system consisting of
  - control hardware (for data acquisition and command output), and
  - control software (for implementation of the control algorithm);
- a signal transfer system for the transport of
  - power, and
  - measurement signals.

3.1. Transmissions

Since servo motors typically provide high speeds with low torques, transmissions are often necessary to transform these quantities into the required opposite combination: low speeds with high torques. On the other hand, transmissions are also an important (additional) source of joint friction, elasticity, and backlash.

To eliminate these drawbacks, attempts have been made to develop actuation systems which allow direct connection of the motor to the joint without the use of any transmission element. The use of such *direct-drive* actuation systems is not yet popular for industrial manipulators, mainly because of the control complexity; due to the absence of reduction gears, the nonlinear terms in the dynamic model can no longer be neglected (see Section 2).

For the RRR-robot, however, this complexity is exactly what we want. Furthermore, the application of direct-drives also complies with an additional design goal: modern state-of-the-art techniques.

3.2. Motor types

Motor types used for the actuation of joint motions can be classified into three groups:

1. Pneumatic motors,
2. Hydraulic motors, and
3. Electric motors.

Of this groups the following servos are typically used for direct-drive applications:

- hydraulic motors, and
- electrical motors:
  - Variable Reluctance Stepper (VRS) motors,
  - Direct-Current (DC) motors, and
  - Brushless Direct-Current (BDC) motors.

Pneumatic motors are not suitable for applications where continuous motion control is of concern due to their unavoidable air compressibility errors. They are mainly used in simple pick-and-place applications and for opening and closing motions of the jaws in a gripper tool.

Asynchronous induction motors are typically suited to deliver high power (> 1kW). Moreover, they are difficult to control and therefore not yet popular for servos.

Hydraulic motors Compared to electrical motors, hydraulic motors have several advantages. They:

- can achieve much higher torques at low velocities,
- have an excellent power-to-weight ratio, and
- are self-lubricated and self-cooled by the circulating fluid.

However, they also present the following drawbacks:

- need for a hydraulic power station,
- temperature dependent dynamics,
- need for regular maintenance, and
- pollution of the working environment due to oil leakage.

The last drawback is a significant problem, especially in combination with the specified unconstrained rotation in each joint. Since the hydraulic lines (conducting the power signals) must pass through a joint without rotational constraints, leakage is difficult to avoid.

Mainly because of this last problem, a choice was made to use electrical motors.

Variable-Reluctance Stepper motors The VRS motor is an induction type stepping motor. Both stator and rotor consist of laminated steel with a high number of opposing teeth; only the stator has (phase) windings. Torque is generated from the variation of the air gap due to the difference in teeth pitch on the rotor and the stator.

In principle no measurement of the motor-shaft angle is required, and the rotor position can be controlled by suitable excitation sequences. Together with the absence of permanent magnets, this results in simple and cheap actuators. However, the stepping nature of this motor type causes a poor position accuracy, vibrations, and a significant torque ripple. Such inconveniences confine the use of stepper motors to applications, where low-cost implementation prevails over the need for accuracy and high dynamic performance.

With the use of a controller (and motor-shaft position feedback), the mentioned problems can be partly solved; torque control however, is difficult to realize.

Direct-Current motors Like the regular DC motor, the direct-drive version consists of a stator[2] which generates a permanent magnetic field (by ferromagnetic ceramics or rare earths), and a winded rotor which is powered via brushes and commutators.

[2] Brushed DC motors come in a wide range of configurations, this configuration (permanent magnet stator and winded rotor) is most common in direct-drive applications.

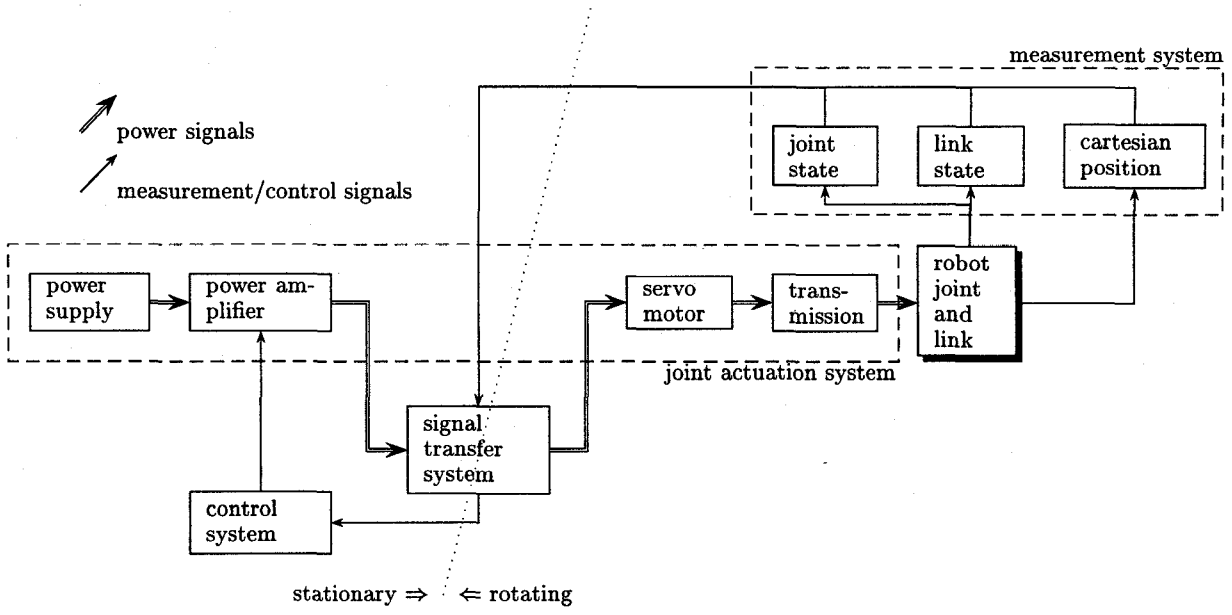

Figure 2: A possible functional lay-out for one of the RRR-robot's links; especially the position of the signal transfer system relative to the joint actuation system may vary (e.g., the power amplifier could also be placed on the rotating link, so right from the signal transfer system.

The design goal of a direct-drive DC motor is to maximize the output torque (the product of the torque constant and the rotor current) rather than power. Since the motor constant is proportional to the inductance, L, direct-drive motors often have a bulky or sometimes 'pancake' like appearance because a large inductance requires a considerable motor volume (and mass): $L \sim$ (length) $\times$ (diameter)^2. Maximizing the current meets with an important limitation of the DC motor in general: mechanical commutation. At the brush and commutator, large sparks can occur especially in combination with a large inductance. These sparks cause the brush to wear quickly and cause unwanted noise. Furthermore, the brush mechanism increases mechanical friction.

Brushless Direct-Current motors In a brushless DC motor, mechanical commutation has been replaced with electronic commutation. Unlike conventional DC motors, the rotor consists of permanent magnets, while the stator consists of several phase windings. The commutation of currents is accomplished by measuring the rotor position using a position sensor.

The elimination of brush and commutator allows an improvement of motor performance in terms of higher torques and less material wear, and is therefore the main reason for using BDC motors.

The inversion between the functions of stator and rotor leads to further advantages. The presence of a winding on the stator instead of the rotor, facilitates heat disposal. The absence of a rotor winding allows construction of more compact rotors, which in turn have a lower moment of inertia. As a result, the size of a BDC motor is smaller than that of a regular DC motor of the same power.

The superiority of the brushless motor, though, comes at a cost: the rotor position must be detected or measured, and fed back to the power amplifier (typically a DC-to-AC converter). However, if such an internal sensor is accurate enough for robot control purposes, no additional joint position sensors are necessary, and the construction becomes more compact.

Summary Considering the advantages of BDC motors, a choice is made to use brushless direct-drive motors for all joints. Preferably, the internal sensors should be used for the robot control.

3.3. Servo sizing

Choosing appropriate servos for the RRR-robot is an iterative problem, since, even for brushless direct-drive servos, the torque-to-mass ratio is small. So, as a result of the required torques, each motor has also a significant mass. To accelerate these masses, even larger motors may be necessary.

To aid the motor choice, a rigid-manipulator model of the RRR-robot is used. The aim is to find three motors with the right combination of mass, torque and angular velocity; at least one link should have an ratio r of 50 % or more at the largest possible angular velocity.

Rigid-body model The dynamic model of a rigid robot with three revolute joints, is derived with the Euler-Lagrange formulation, using the Denavit-Hartenberg matrix representation [3] to describe the spatial displacement between the neighboring link coordinate frames. The choice of these coordinate frames for the RRR-robot is shown in Fig. 3. The position and orientation of frame O_i with respect to frame O_{i-1} is completely specified by the parameter vectors of Table 1. Three of these four parameters ($\underline{a}$, $\underline{d}$ and $\underline{\alpha}$) are constant, and only depend on the geometry of the robot. The resulting coordinate transformation $T_0^n(\underline{a}, \underline{d}, \underline{\alpha}, \underline{q})$ from the link frame O_n to

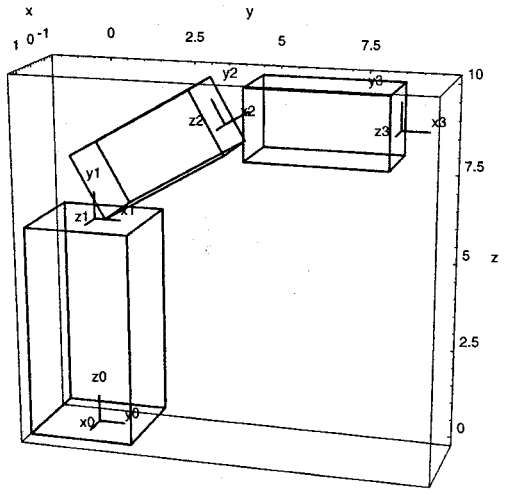

Figure 3: Orientation of the coordinate frames: O_0 is placed at the center-base of link 1, O_i at the end of link i. The center of each servo motor (not shown) is located at O_0, O_1 and O_2 parallel to the z-axis.

Table 1: Denavit-Hartenberg parameters for the RRR-robot based on the coordinate frames of Fig. 3; l_i is the length of link i measured from O_{i-1} to O_i, d_i is the offset of each link along the z-axis needed for unconstrained rotation, and q_i is the rotation angle of motor i.

parameters link		1	2	3
a_i	$= D(O_{i-1}, O_i)$ along x_i	0	l_2	l_3
d_i	$= D(O_{i-1}, O_i)$ along z_{i-1}	l_1	d_2	d_3
α_i	$= \angle(z_{i-1}, z_i)$ about x_i	$\frac{\pi}{2}$	0	0
q_i	$= \angle(x_{i-1}, x_i)$ about z_{i-1}	q_1	q_2	q_3

the base coordinate frame O_0 is given by the product of homogeneous transformation matrices, i.e.,

$$T_0^n(\underline{q}) = A_0^1 A_1^2 \dots A_{n-1}^n \tag{7}$$

where

$$A_{i-1}^i(\underline{q}) = \begin{bmatrix} \cos(q_i) & -\cos(\alpha_i)\sin(q_i) & \sin(\alpha_i)\sin(q_i) & a_i\cos(q_i) \\ \sin(q_i) & \cos(\alpha_i)\cos(q_i) & -\sin(\alpha_i)\cos(q_i) & a_i\sin(q_i) \\ 0 & \sin(\alpha_i) & \cos(\alpha_i) & d_i \\ 0 & 0 & 0 & 1 \end{bmatrix}$$

So all link properties (such as the center of gravity and the link or motor inertia) defined in their own link coordinates, can be expressed in base coordinates. Combining the Denavit-Hartenberg representation and the Lagrange formulation [3, 2], the dynamics of (1) can be derived in a systematic way. The mass matrix M, for example, can be written as

$$M_{ik} = \sum_{j=\max(i,k)}^{n} \mathrm{tr}\left\{ \frac{\partial T_0^j}{\partial q_k} J_j \left(\frac{\partial T_0^j}{\partial q_i} \right)^T \right\} \tag{8}$$

where J_j is the combined inertia matrix of link j and motor j. For optimal flexibility Mathematica [6] was

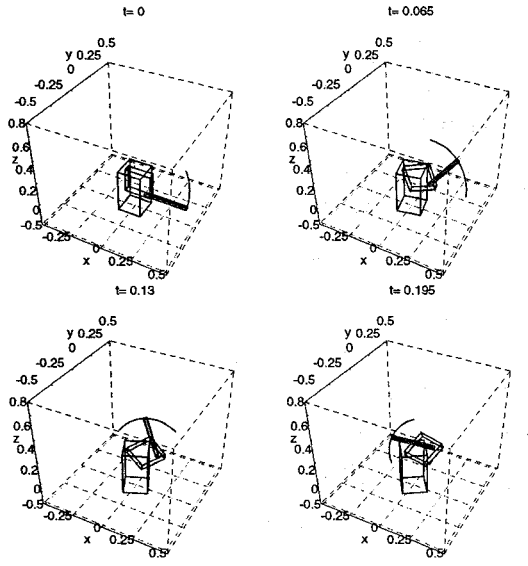

Figure 4: A wire-frame 'animation' of the initial design. All quantities are in SI-units: t in [s], and x, y, z in [m].

Table 2: Main system parameters used in evaluation model. The links are assumed to be rectangular aluminum beams. The motor data are taken from the Dynaserv series of Litton Precision Products.

parameters link/joint		1	2	3
link length	[m]	0.5	0.2	0.2
link mass	[kg]	9.86	1.21	0.73
motor mass	[kg]	12	7.5	5.5
motor inertia	[kg m^2]	0.023	0.015	0.012
max. torque	[Nm]	60	30	15

used to generate the resulting equations of motion. Implementing (8) in this symbolic manipulation package is straightforward:

```
Mik[i_,k_] := Sum[ tr[
D[T[j],q[[k]]] .J[j]. Transpose[ D[T[j],q[[i]]] ]],
{j,Max[i,k],n} ]
```

Initial design Based on an initial design sketch a rough estimate was made for the link parameters (i.e., dimensions and material) leading to the main system parameters shown in the upper part of Table 2. To illustrate this initial design the kinematic relations were used to draw the simplified wire-frame picture of Fig. 4. After choosing an appropriate motion pattern, i.e., with a high integral ratio r, a commercial motor can be evaluated by substituting its mass and rotor inertia.

With the Dynaserv series of BDC motors of Litton Precision Products (see the motor data in the lower part of Table 2) the main design requirement, maintaining high Coriolis and centrifugal forces, has been met. This is illustrated in Fig. 5 with on the left the torques required to realize a stationary motion pattern (without inertia effects because $\ddot{\underline{q}}_i = 0$, so with large ratios r_i)

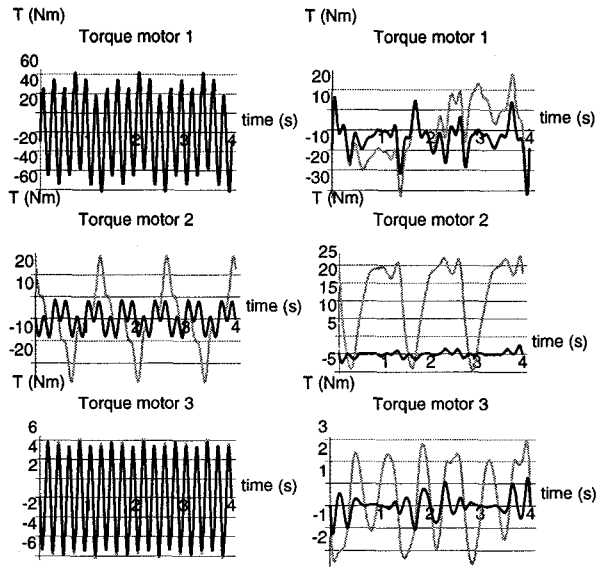

Figure 5: Required motor torques (thick gray lines) to realize a chosen motion pattern without accelerations (on the left) and with accelerations (on the right). The contribution of the Coriolis and centrifugal torques is shown with a thick black line.

$\underline{q}_{\text{stat}} = [\pi\ t, 2/3\pi\ t, 3\pi\ t]^T$ [rad] ; on the right are the torques required to realize a motion pattern with accelerations: $\underline{q}_{\text{dyn}} = [\sin \pi/2\ t, \sin 3/2\pi\ t, \sin 3\pi\ t]^T$ [rad]. Both motion patterns are chosen to achieve the maximum torque of one or more motors.

Evaluation of (2) for each link yields $r = [1, 0.39, 1]$ for $\underline{q}_{\text{stat}}$ and $r = [0.51, 0.03, 0.20]$ for $\underline{q}_{\text{dyn}}$. So for both motion patterns, the Coriolis and centrifugal component of motor 1 is above the required 50% of the total torque.

4. Closed loop simulation

The rigid-robot model with the selected servos (Table 2) is used to simulate the dynamics of tracking a desired trajectory $\underline{q}_d$ with a Passivity-based Computed Torque Controller [2], i.e.,

$$\underline{u} = \underline{\tau} = M\ddot{\underline{q}}_d + C\dot{\underline{q}}_d + \underline{g} + K_D\dot{\underline{e}} + K_P e \qquad (9)$$

with $\underline{e} = \underline{q}_d - \underline{q}$ the tracking error, and K_D and K_P positive definite feedback matrices. This method exploits the pasivity property of mechanical systems to guarantee asymptotic stability of the closed loop system. Implementing this control law, again, is straightforward:

```
u = limitu[
M . qdes''+ CC . qdes' + g + KD. e' + KP . e,
    {48,20,10} ];
```

Note that the applied motor torque has been limited by a safety margin. The results of this simulation with $\underline{q}_d = [\pi\ t, 3/2\pi\ t - \pi/2, 3\pi\ t]^T$, and initial conditions $\underline{q}(0) = \dot{\underline{q}}(0) = \underline{0}$ [rad] are shown in Fig. 6. The controller parameters and desired trajectory were set to achieve reasonable tracking while slightly saturating the motors.

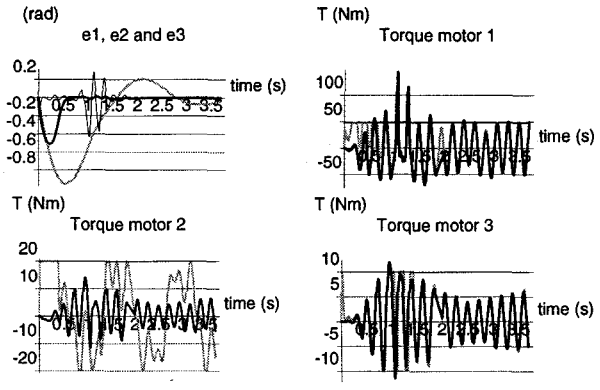

Figure 6: CTC controller: position errors e_1 (thick gray line), e_2 (thick black line) and e_3 (thin black line); and motor torques (total torque with a thick gray line, contribution of Coriolis and centrifugal torques with a thick black line).

5. Discussion

Two important features of the RRR-robot were introduced in order to reach the design goal of large nonlinear dynamic forces: unconstrained rotation in each link (e.g., by using sliprings) and the use of direct-drive servos. Several types of direct-drive servos were discussed and brushless direct-current motors were selected for this application. The iterative dynamic optimization problem of choosing appropriate servos and finding the main dimensions of the construction was solved by using a rigid-robot model, implemented in a symbolic manipulation program, that was used for both open and closed loop simulation studies. The design of the robot is now completed and manufacturing has started. In the near future we expect to report our experiences with this hardware.

References

[1] Lammerts, I., Veldpaus, F., Kok, F., and Van de Molegraft, M. (1993). *Adaptive computed torque computed reference control of flexible robots.* In *ASME 1993 Winter annual meeting*, New Orleans, Louisiana, USA.

[2] Lammerts, I. M. (1993). *Adaptive computed reference computed torque control of flexible manipulators.* Ph.D. thesis, Eindhoven University of Technology.

[3] Lee, C. (1982). *Robots kinematics, dynamics and control. IEEE Computer*, **vol. 15** (no. 12), pp. 62–80.

[4] Van der Linden, G.-W. (1997). *High performance robust manipulator motion control: theory, tools and experimental implementation.* Ph.D. thesis, Delft University of Technology.

[5] Sciavicco, L. and Siciliano, B. (1996). *Modeling and control of robot manipulators.* McGraw-Hill series in electrical engineering. McGraw-Hill, London.

[6] Wolfram, S. (1993). *Mathematica, a System for Doing Mathematics by Computer.* Addison-Wesley Publishing Company.